

---

# THE THERMAL TRANSMISSION BEHAVIOR ANALYSIS OF TWO COAL GANGUES SELECTED FROM INNER MONGOLIA IN CHINA

by

Lixin LI, Yinmin ZHANG\*, Yongfeng ZHANG, Junmin SUN, Ziqiang WANG

Chemical Engineering College, Inner Mongolia University of Technology, Hohhot 010051 China

*The differences in the structure and thermal behavior of two coal gangue samples (Z-1 and Z-2) obtained from Inner Mongolia in China were investigated through thermogravimetry–derivative thermogravimetry (TG-DTG), X-ray diffraction (XRD), and Fourier-transform infrared (FT-IR) spectroscopy. The TG-DTG results indicate that the two coal gangue samples present different dehydroxylation temperatures and loss on ignition values. The mineralogy of the Z-1 sample consisted of kaolinite and quartz, whereas that of the Z-2 sample consisted of kaolinite, boehmite and quartz. The XRD and FT-IR spectra revealed the thermal transmission behavior of the two coal gangue samples when temperature was increased from 300 °C to 1000 °C. The coal gangue samples lost hydration water at a temperature of up to 500°C, and the layer structure collapsed completely as the temperature increased. The typical bands in the FT-IR spectra of the two coal gangue samples are similar, but several differences were observed in the intensity and positions of bands. The intensity of the characteristic bands of boehmite in the samples at 3090 and 3280cm<sup>-1</sup> decreased as the temperature increased, and the bands disappeared at 600 °C. The thermal behavior of the coal gangue samples differed because of impurities and mineralogical compositions.*

**Keywords:** coal gangue, thermal behavior, dehydroxylation, kaolinite, boehmite

## Introduction

Coal is expected to become the predominant fossil fuel in use for at least the next 50 years [1]. However, coal consumption produces a large amount of coal gangue. Coal gangue is the solid waste produced in the process of coal mining and beneficiation, it is sandwiched between coal seam and varies from 10 % to 15 % depending on mining range and geological conditions [2–4]. In China, the total accumulated stockpile of coal gangue has reached 4.5 billion metric tons [5, 6]. Coal gangue can cause serious damage to the environment, including occupying a large amount of land and farmland and polluting the atmosphere and water. Previously, Querol et al. have conducted field and lab study on spontaneously ignited gangue hills in Yangquan in Shanxi province, China and demonstrated the exacerbation of environmental impact on local soil and water body of spontaneous combustion of gangue hills other than long term weathering [7]. Coal gangue contains various

---

44 chemical and mineral compositions, and generally contains large amounts of silica, alumina, clay  
45 minerals and carbonaceous minerals [8–11]. The utilization of coal gangue has elicited much attention  
46 in China in the past decades. The chemical composition of coal gangue varies significantly with  
47 different time horizons, regions and means of mining. The main chemical components of coal gangue  
48 are SiO<sub>2</sub>, Al<sub>2</sub>O<sub>3</sub> and carbon, in addition to TiO<sub>2</sub>, Fe<sub>2</sub>O<sub>3</sub>, CaO, K<sub>2</sub>O, Na<sub>2</sub>O, etc [12–14]. Its mineral  
49 components mainly include clay minerals (kaolinite, sericite), quartz, calcite, pyrite, siderite and  
50 carbonaceous minerals [15, 16]. The most common and dominant clay mineral in coal gangue is  
51 kaolinite. Kaolinite is a 1:1 layered dioctahedral aluminum silicate that belongs to the kaolin group of  
52 minerals. The 1:1 layer structure consists of tetrahedral silica units stacked together with octahedral  
53 alumina units [17, 18]. The folded layers are connected by van der Waals forces and strong hydrogen  
54 bonds involving both Al and Si groups (Al–O–H–O–Si).

55 The technological applications of coal gangue are based on its physical and chemical  
56 properties, structure, composition, and thermal behavior [19-21]. Coal gangue is an important and  
57 useful industrial byproduct because of its properties, such as minimal impurities and low carbon  
58 content. Coal gangue with minimal impurities has been used utilized in the manufacture of building  
59 products, porcelain, refractories, etc [22]. Most of the studies in recent years focused on structural and  
60 textural changes in coal gangue. Thermal treatment can change the physical and chemical properties of  
61 coal gangue and provides some information about the thermal evolution of coal gangue because  
62 several physico–chemical properties of coal gangue, such as particle size, surface area, and mineralogy  
63 are significantly affected by thermal treatment [23]. Yuanyuan Zhang et al thought that the feedstock  
64 properties (combustible matter, mineral matter) of coal gangue are different depending on source, coal  
65 rank, and coal mining technique and washing technology and feedstock properties affected the change  
66 of activation energy with conversion values[24]. High-ash coal gangue combustion behavior is not  
67 only influenced by combustible matter but also by mineral matter. This effect is most probably due to  
68 the heat absorption of mineral matter[25-27]. There is little information about the research of the  
69 thermal behavior of coal gangue from different coal seam. Thermal treatment can provide some  
70 information about thermal evolution of coal gangue and is necessary for its further application,  
71 especially in the filler industry.

72 This study investigates the structure and behavior of thermal treatment of two coal gangue  
73 samples obtained from Inner Mongolia in China through thermogravimetry–derivative  
74 thermogravimetry (TG-DTG), X-ray diffraction (XRD), and Fourier transform infrared  
75 spectroscopy(FT-IR). The purpose of the study is to investigate the structural evolution of the  
76 chemistry and mineralogy of the two coal gangue samples obtained from different coal seams during  
77 thermal treatment.

## 78 **Experimental**

### 79 **Materials and methods**

80  
81  
82  
83 Two main types of coal gangue exist in the Inner Mongolia coal field: one type is from  
84 the roof of the coal seam, and is mainly composed of mud stone, clay or shale powder sandstone. The  
85 other one is from tonstein in the coal seam, and is mainly composed of mud stone, carbonaceous mud  
86 stone, clay and rock. Two coal gangue sample was collected through drilling hole from the single

87 vertical direction. Samples of the same borehole contain roof and tonstein coal gangue. Two coal  
 88 gangue samples were obtained from the roof (Z-1) and tonstein (Z-2) of coal mines multiple boreholes  
 89 in Inner Mongolia. The two coal gangue samples were ground to 200 meshes with a jaw crusher and  
 90 sieved to a particle size of below 100  $\mu\text{m}$ . The treated coal-gangue samples were heated at 300  $^{\circ}\text{C}$ ,  
 91 400  $^{\circ}\text{C}$ , 500  $^{\circ}\text{C}$ , 600  $^{\circ}\text{C}$ , 700  $^{\circ}\text{C}$ , 800  $^{\circ}\text{C}$ , 900  $^{\circ}\text{C}$  and 1000  $^{\circ}\text{C}$  for 2h at a rate of 10  $^{\circ}\text{C min}^{-1}$  in a  
 92 muffle furnace under an air atmosphere. Related tests and experiments were then conducted. The main  
 93 chemical component and loss on ignition of the two coal gangue samples are shown in Tab. 1.

94

95 **Table 1. Chemical composition of two coal gangue samples from Inner Mongolia**

96

Coal gangue sample	SiO <sub>2</sub> (%)	Al <sub>2</sub> O <sub>3</sub> (%)	Fe <sub>2</sub> O <sub>3</sub> (%)	TiO <sub>2</sub> (%)	Na <sub>2</sub> O (%)	K <sub>2</sub> O (%)	MgO (%)	Loss on ignition (%)
Z-1	44.313	31.260	0.266	0.820	0.056	0.051	0.050	22.182
	42.264	30.271	0.176	0.746	0.041	0.052	0.043	24.410
	43.214	32.312	0.184	0.823	0.061	0.046	0.053	21.307
Z-2	33.680	37.569	0.266	0.649	0.076	0.070	0.056	26.610
	35.142	38.571	0.242	0.721	0.064	0.062	0.049	24.148
	32.734	37.531	0.245	0.623	0.061	0.073	0.043	26.648

97

## 98 **Characterization**

99

100 The phase compositions of the raw coal gangue samples before and after thermal  
 101 treatment were investigated through XRD analysis by using a diffractometer(D/MAX 2500 PC,  
 102 Rigaku) equipped with a Cu target, K $\alpha$  radiation source, and slit system, at a scanning speeds of 4 $^{\circ}$   
 103  $\text{min}^{-1}$ , and scanning range of 2.5-60 $^{\circ}$  (2 $\theta$ ), The tube voltage was 40kv, and the tube current was 40 mA.

104 FT-IR was conducted with a Thermofisher Nicolet6700 spectrometer. The samples were  
 105 prepared at potassium bromide (KBr) pellets and then ground in an agate mortar, The mixture was  
 106 pressed into a pellet for the transmittance infrared spectroscopic measurements. The FI-IR spectra of  
 107 the prepared samples between 400 and 4000  $\text{cm}^{-1}$  were recorded.

108 TG-DTG measurements were carried out with Switzerland Mettler Toledo  
 109 TGA/DSC1/1600HT. The two coal gangue samples were heated from ambient temperature to up to  
 110 1100  $^{\circ}\text{C}$  at a heating rates of 10  $^{\circ}\text{C min}^{-1}$  under air atmosphere.

111 The morphology of the raw and the calcined coal gangue was observed by a cold field  
 112 emission scanning electron microscope (SEM, S-4800, Hitachi). During the observation, an  
 113 accelerating voltage of 15kV was selected, and the resolution was of  $\pm 2$  nm.

114

## 115 **Results and Discussion**

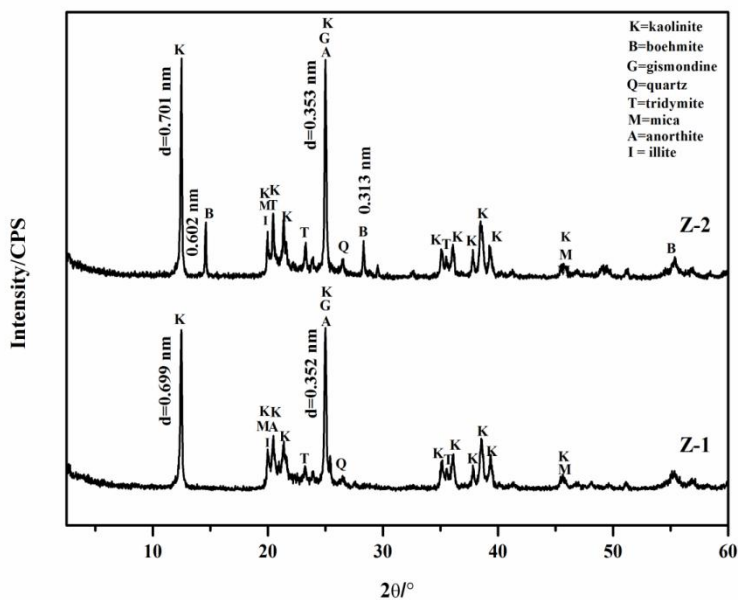
116

### 117 **XRD**

118

119 The XRD patterns of the two raw coal gangue samples are shown in Fig. 1. The major  
 120 mineralogical composition of the Z-1 sample is kaolinite and quartz. In addition, The XRD patterns  
 121 the two raw coal gangue also contains weak diffraction peaks of tridymite, mica, anorthite, and

122 gismondine, etc. The pattern of the Z-1 sample presents several typical strong diffraction peaks of  
 123 kaolinite ( $\text{Al}_2\text{O}_3 \cdot 2\text{SiO}_2 \cdot 2\text{H}_2\text{O}$ ) at  $2\theta=12.6^\circ$  and  $25^\circ$ , and the values of these diffractions are 0.701 and  
 124 0.353 nm because of the diffraction of the (001) and (002) crystal planes, respectively. The three  
 125 diffraction peaks with values of 0.407, 0.431, and 0.413 nm at  $2\theta=22^\circ-25^\circ$  are due to the diffraction of  
 126 (020), (110), and (111) crystal surface reflection, respectively. The diffraction peak with a value of  
 127 0.350 nm at  $2\theta=26.7^\circ$  is attributed to quartz [28]. The mineral components of the Z-1 sample are  
 128 relatively pure kaolinite according to the diffraction peaks. The major mineralogical composition of  
 129 the Z-2 sample is kaolinite and quartz. The identical peak intensity and position are also shown in  
 130 diffractogram of the Z-2 sample. In the pattern of the Z-2 sample, the characteristic diffractions peaks  
 131 with values of 0.602, 0.313, and 0.165 nm at  $2\theta=14.7^\circ$ ,  $28^\circ$ , and  $55^\circ$  are attributed to boehmite [29,  
 132 30], indicating that boehmite ( $\gamma$ -aluminum oxihydroxide  $\text{AlOOH}$ ) is also the main mineral components.  
 133 Boehmite is usually a component of bauxite and a mineral uncommon in coal gangue. The boehmite  
 134 locating in the bottom layers of coal gangue are formed by desilication effect of kaolinite under the  
 135 action of humic acid. These results reveal the high content of aluminum in the Z-2 sample, thus the  
 136  $\text{SiO}_2/\text{Al}_2\text{O}_3$  molar ratio is less than the theoretical value. Boehmite is enriched in the Z-2 sample. The  
 137 molar ratio of  $\text{SiO}_2/\text{Al}_2\text{O}_3$  in the Z-1 sample is less than 2, whereas the molar ratio of  $\text{SiO}_2/\text{Al}_2\text{O}_3$  in the  
 138 Z-2 sample is greater than 2, thus indicating the high aluminum content and abundant aluminum  
 139 minerals in the Z-2 sample. In the pattern of the sample Z-1, the diffraction peak attributed to quartz at  
 140  $2\theta=26.7^\circ$  is intense, which indicates that sample Z-1 contains more quartz than sample Z-2. The  
 141 mineral components of the Z-1 sample are relatively pure kaolinite according to the diffraction peaks.  
 142 These results are consistent with the chemical analysis results.

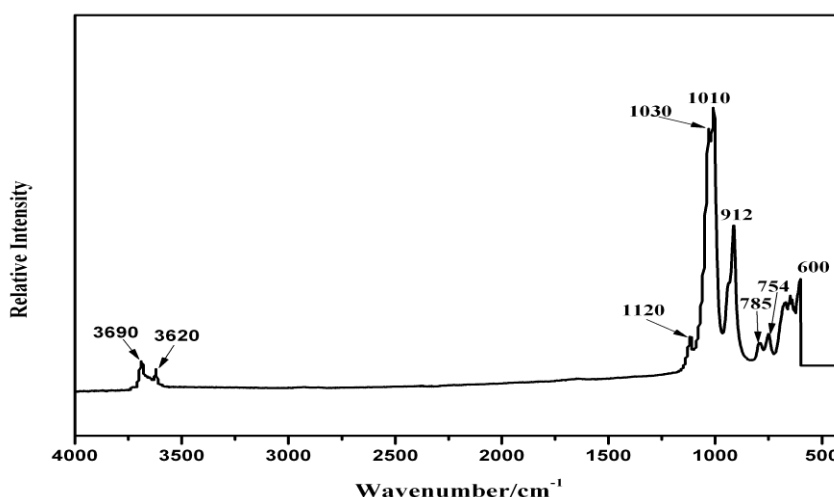


143  
 144 **Fig. 1 XRD patterns for two raw coal gangue**  
 145

146  
 147 **Infrared spectroscopy**  
 148

149 The FT-IR spectroscopy can reveal the molecular structure of coal gangue. Coal gangue is  
150 mainly composed of kaolinite. The infrared spectra of kaolinite mainly include characteristic  
151 absorption bands of Si-O, -OH, and H-O-H. which contain typical stretching vibration modes of  
152 -OH and H-O-H in the high-frequency region (3600–3400  $\text{cm}^{-1}$ ) and bending vibration modes of  
153 Si-O, Al-O groups, and hydroxyl groups in the low frequency region (1600–400 $\text{cm}^{-1}$ ) [31]. The FT-IR  
154 spectra of the two coal gangue samples are shown in Figs. 2 and 3. Differences in the position and  
155 intensity of the H-O-H, -OH, Si-O, and Al-O group vibration modes were observed. These  
156 differences may be due to the variations in composition and impurities. Two obvious and similar bands  
157 were observed for the two coal gangue samples in the 3500–4000  $\text{cm}^{-1}$  region. The bands at 3620  $\text{cm}^{-1}$   
158 and 3690  $\text{cm}^{-1}$  are approximately attributed to the inner hydroxyl stretching vibration peak and outer  
159 hydroxyl stretching vibration. Three bands (3690, 3620  $\text{cm}^{-1}$ ) in the OH stretching region are attributed  
160 to kaolinite with mostly Al in the octahedral position. The absorption peak at 912  $\text{cm}^{-1}$  is attributed to  
161 Al-OH bending vibration [32]. The bands at 1030 and 1120  $\text{cm}^{-1}$  are assigned to Si-O-Si stretching  
162 vibrations, indicating that the existence of kaolinite, tridymite, illite and quartz in coal gangue, in  
163 agreement with the XRD results.

164 Fig.3 shows the FT-IR spectra of the Z-2 sample. In the high wavenumber region, in  
165 addition to the hydroxyl vibration characteristic bands of kaolinite in the range of 3000–3300  $\text{cm}^{-1}$ , the  
166 bands at 3280 and 3090  $\text{cm}^{-1}$  are associated with the stretching vibration band mode of the hydroxyl of  
167 boehmite, and the bands at 746 and 642 $\text{cm}^{-1}$  are associated with the characteristic bands of boehmite  
168 that are attributed to the superposition band of Al-O stretching vibration and bending vibration  
169 absorption of kaolinite and boehmite [33]. The band at 1610  $\text{cm}^{-1}$  is attribute to Si-O-Si asymmetric  
170 stretching vibrational and O-Si-O stretching vibration mode [34], indicating that the existence of  
171 illite. The result corresponds to the result of XRD.



188 **Fig. 2 FT-IR spectra for Z-1 coal gangue**

192  
193  
194  
195  
196  
197  
198  
199  
200  
201  
202  
203  
204  
205  
206  
207  
208  
209  
210  
211  
212  
213  
214  
215  
216  
217  
218  
219  
220  
221  
222  
223  
224  
225  
226  
227  
228  
229  
230  
231  
232  
233  
234

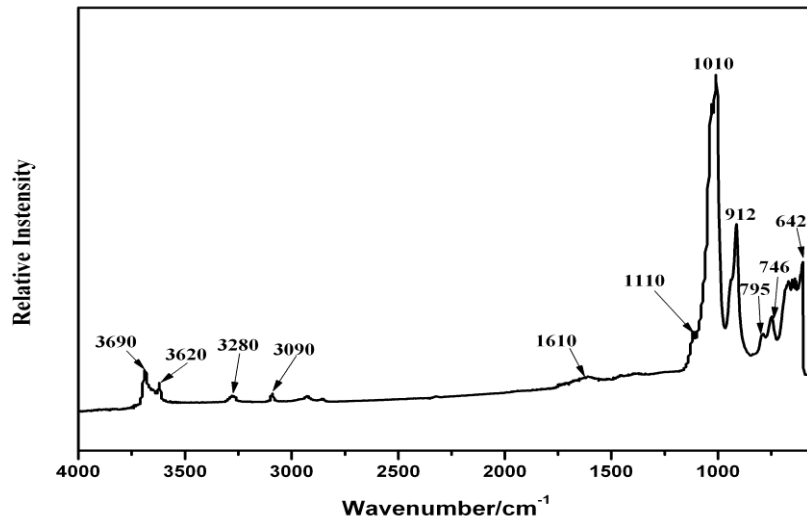
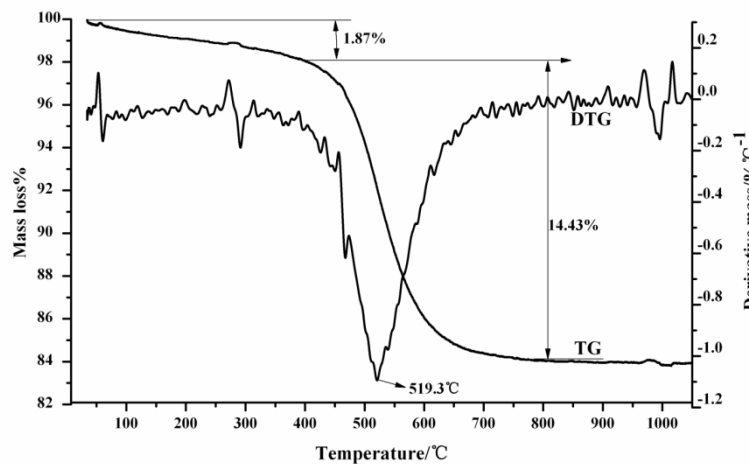


**Fig. 3 FT-IR spectra for Z-2 coal gangue**

### Thermal analysis

The TG–DTG curves of samples Z-1 and Z-2 are shown in Figs. 4 and 5. An endothermic peak exists at approximately 100 °C in the Z-1 sample, with a mass loss of 1.87 %, The peak is attributed to the adsorbed water in the TG–DTG curves of the Z-1 sample in Fig. 4. The endothermic peak presented at 519.3 °C with a mass loss of 14.43% is associated with the dehydroxylation of coal gangue. However, the endothermic peak presented at 501.5 °C with a mass loss of 22% is associated with the dehydroxylation of the Z-2 sample in Fig. 2. The theoretical loss of the structural water of kaolinite is 14.4 %. The loss on ignition of the Z-2 sample is larger than that of the Z-1sample. The mass loss of Z-2 sample is larger than the theoretical value of the structure of water in kaolinite, which indicates that dehydroxylation reaction and carbon loss of kaolinite and boehmite occurred [16], This result is in agreement with the loss on ignition results of the two coal gangue samples. The differences in the thermal behaviors of the two coal gangue samples were distinct, which indicates that mineral compositions exerted a significant influence on the thermal behavior of the samples.



235  
236  
237  
238  
239  
240  
241  
242  
243  
244  
245  
246  
247  
248  
249  
250  
251  
252  
253  
254  
255  
256  
257  
258  
259  
260  
261  
262  
263  
264  
265  
266  
267  
268  
269  
270  
271  
272  
273  
274  
275  
276  
277

**Fig. 4 TG-DTG-DSC curves for the Z-1 coal gangue**

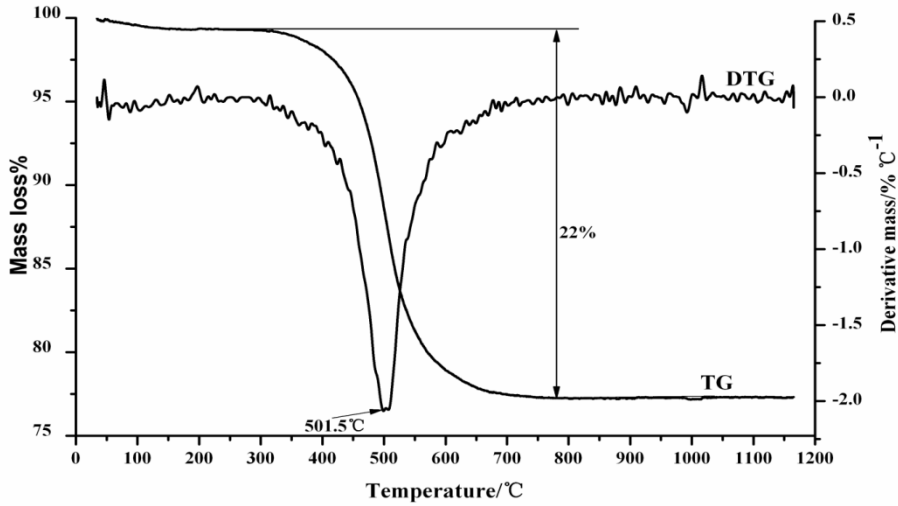
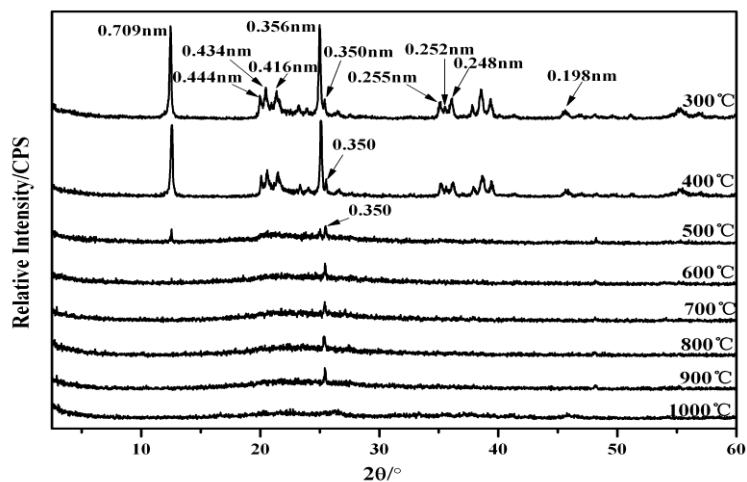


**Fig. 5 TG-DTG-DSC curves for the Z-2 coal gangue**

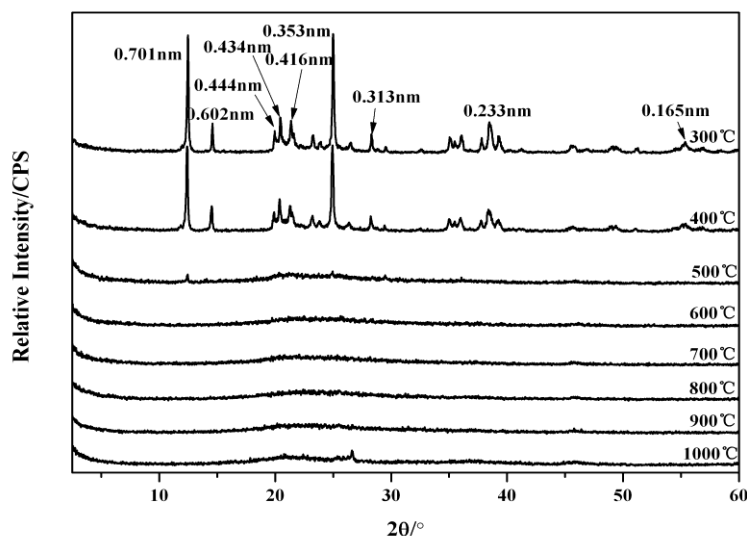
**Mineral transformation and structural evolution of the two coal gangue samples during calcination**

The XRD patterns of two thermally treated coal gangue samples calcined at 300 °C to 1000 °C are shown in Figs. 6 and Fig. 7. The diffraction peak shape of the two samples calcined at 300 °C and 400 °C is similar to that of the two raw coal-gangue samples. The change in the XRD diffractogram of the Z-1 sample at different temperatures is shown in Fig. 6. The diffraction peak with a value of 0.709 nm at  $2\theta=12.4^\circ$  gradually weakened as the temperature increases. At a calcination temperature of 600 °C, the diffraction peaks of kaolinite completely disappeared through the removal of the inner hydroxyl structure, which may be due to the destruction of the crystal face (001) the formation of an amorphous substance, and transformation of kaolinite to metakaolinite[4, 16]. The diffraction peak with a value of 0.350 nm at  $2\theta=25^\circ$  is attributed to quartz. The diffraction peak attributing to kaolinite, gismondine, mica, anorthite etc at 20-40°C basically disappeared. The diffraction peaks of quartz still exist as the temperature increases, which could be attributed to the generation of active SiO<sub>2</sub> through the decomposition of clay minerals, such as metakaolinite and illite. Fig. 7 shows the diffraction patterns of the Z-2 sample at different temperatures. The diffraction peak with a value of 0.701nm at  $2\theta=12.6^\circ$  gradually weakened as the temperature increased and disappeared at 600 °C. The characteristic diffractions peaks of boehmite with values of 0.602 and 0.313 nm also gradually weakened and disappeared at 700 °C, thus revealing the destruction of the crystal face of boehmite and the formation of an amorphous substance. The diffraction peak at 20-40°C basically disappeared and the diffraction peaks of quartz also disappeared, indicating that sample Z-1 contains more quartz than sample Z-2. The result corresponds to the result of XRD analysis of raw samples.

278 The crystallinity of two gangue was gradually decreased and the symmetry changed worse  
279 as the temperature increases, which causing diffraction peak broaden and weaken. The coal gangue  
280 has transformed from the crystalline to amorphous state.



293  
294  
295  
296 **Fig. 6 XRD patterns for Z-1 coal gangue sample heated at different temperatures**



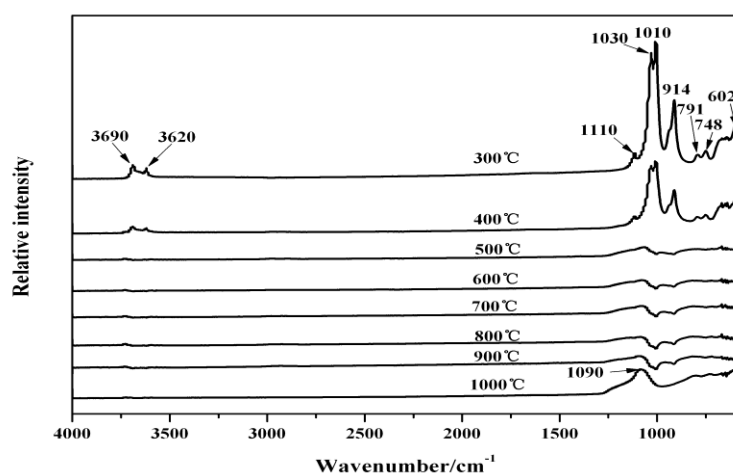
310  
311  
312 **Fig. 7 XRD patterns for Z-2 coal gangue sample heated at different temperatures**

313  
314 The FT-IR spectra of the Z-1 sample at different temperatures are presented in Fig. 8. The  
315 intensities of the two bands at 3690 and 3620  $\text{cm}^{-1}$  gradually decreased, and the bands disappeared at  
316 700  $^{\circ}\text{C}$  as the temperature increased in the 3000–4000 $\text{cm}^{-1}$  region, This result indicates that the  
317 hydroxyl groups of coal gangue were removed compared with those in uncalcined coal gangue. The  
318 intensity of the bands at 914  $\text{cm}^{-1}$  gradually decreased, and the band disappeared at 800 $^{\circ}\text{C}$ , This result  
319 indicates that the breakages of Al–OH as the temperature increased. The intensity of the bands at 1110,  
320 1030, and 1010  $\text{cm}^{-1}$  also gradually weakened and presented a wide band at 1090 $\text{cm}^{-1}$  as the

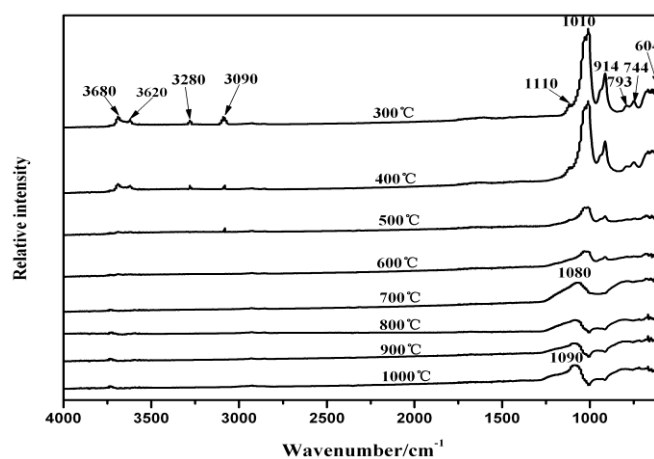


321 temperature increased. This result indicates that the dehydration reaction of illite and kaolinite result in  
322 metakaolinite [35, 36]. These results are associated with the depolymerization and collapse of the  
323 tetrahedral silica structure [37]

324 The FT-IR spectra of the Z-2 sample at different temperatures are presented in Fig. 9. The  
325 changes in high wavenumber are similar to those of the Z-1 sample, and the changes in the bands are  
326 also attributed to the evolution of the hydroxyl group. The bands at 1110 and 1010  $\text{cm}^{-1}$  gradually  
327 weakened as the temperature increased, and a wide band emerged when the temperature was 700  $^{\circ}\text{C}$ ,  
328 which indicates the generation of new substances. The bands at 3280 and 3090  $\text{cm}^{-1}$  gradually  
329 weakened with the increase in temperature and disappeared at 600  $^{\circ}\text{C}$ , indicating that the hydroxyl of  
330 boehmite of in the Z-2 sample was removed as the temperature increased. The intensity of the bands at  
331 793 and 744  $\text{cm}^{-1}$  also gradually weakened with the increase in temperature. The absorption peak at  
332 1090  $\text{cm}^{-1}$  became wider, indicated the generation of new substances. These results are associated with  
333 the dehydroxylation and collapse of the layer structure.

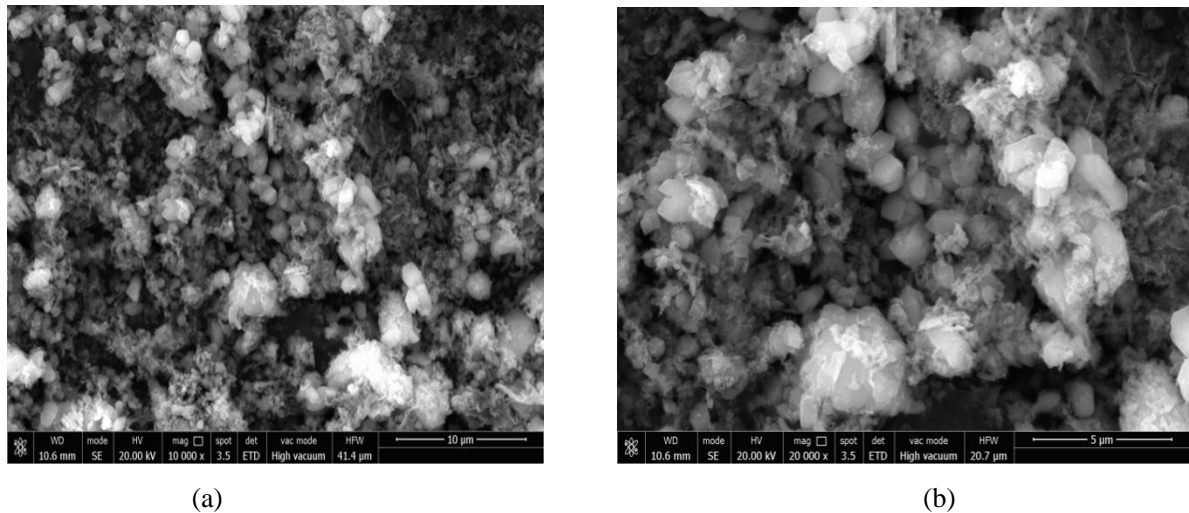


349 **Fig. 8 FT-IR spectra for Z-1 samples heated at different temperatures**



364 **Fig. 9 FT-IR spectra for Z-2 samples heated at different temperatures**

365  
366 The SEM images of the coal gangue calcined at 800 °C are presented in Figs 10 and 11.  
367 Two coal gangue have no obvious difference from the SEM images. The microstructure of two coal  
368 gangue presented uniform and loose size distribution. The structure turns to irregular and porous when  
369 coal gangue heated at 800°C ( in Fig.10 (a) (b) ), which may be caused by the dehydroxylation of  
370 kaolinite and phase change to metakaolin. Calcined coal gangue is basically loose because of the  
371 component volatilization and fame expansion.



385  
386 **Fig. 10 FT-IR spectra for Z-1 and Z-2 samples heated at 800°C**

387 (a) Z-1 coal gangue (b) Z-2 coal gangue

388  
389 **Conclusion**

390 TG-DTG, XRD, and FT-IR spectroscopy were utilized to study the difference in the  
391 structure and thermal behavior of two coal gangue samples obtained from Zhungeer. The TG-DTG  
392 data indicate that the two samples have different dehydroxylation temperature and loss on ignition  
393 values. The mineralogy of the Z-1 sample consist of kaolinite and quartz, whereas that of the Z-2  
394 sample consist of kaolinite, quartz, and boehmite, The Z-2 sample contains high aluminum content  
395 and abundant aluminum minerals, and Z-1sample contains more quartz than the sample Z-2 sample.  
396 This result corresponds to the TG-DTG data. The XRD and FT-IR spectra revealed that the structural  
397 changes in the two coal gangue are due to impurities and mineralogical compositions when  
398 temperature is increased from 300 °C to 1000 °C. The hydroxyl groups of the two coal gangues were  
399 removed at 700 °C. The typical bands in the FT-IR spectra of the two coal gangue samples are similar,  
400 but several differences in positions and intensities were observed. The microstructure of calcined coal  
401 gangue presented uniform and loose size distribution. The results of this work can provide theoretical  
402 basis for extraction of aluminum in coal gangue from Inner Mongolia.

403  
404 **Acknowledgments**

405 This work was financially supported by National Natural Science Foundation of China (51604158).

---

407 **Nomenclature**

408 *TG* – thermogravimetry [%]

409 *DTG* – derivative thermogravimetric analysis [% · K]

410

411 **References**

- 412 [1] Chen, X.Y., et al., Thermal analyses of the lignite combustion in oxygen-enriched atmosphere, *Thermal*  
413 *science*, 19(2015), 3, pp. 801-811
- 414 [2] Liu, H.B., Liu Z.L., Recycling utilization patterns of coal mining waste in China, *Resources Conservation*  
415 *& Recycling*, 54 (2010), 12, pp. 1331–1340
- 416 [3] Zhang, Y.Y., et al., Co-combustion and emission characteristics of coal gangue and low-quality coal.  
417 *Journal of Thermal Analysis & Calorimetry*. 120 (2015), 3, pp. 1883-1892
- 418 [4] Cao, Z., et al., Effect of calcination condition on the microstructure and pozzolanic activity of calcined coal  
419 gangue, *International Journal of Mineral Processing*, 146 (2016), pp. 23-28
- 420 [5] Ye, J.W., et al., Hazards and comprehensive utilization of coal gangue, *China Resources*  
421 *Comprehensive Utilization*, 28(2010), 5, pp.32–34
- 422 [6] Li, Y., et al., Improvement on pozzolanic reactivity of coal gangue by integrated thermal and chemical  
423 Activation, *Fuel*. 109 (2013), 7, pp.527–533
- 424 [7] Querol X, Izquierdo M, Monfort E, et al. Environmental characterization of burnt coal gangue banks at  
425 Yangquan, Shanxi Province, China[J]. *International Journal of Coal Geology*, 2008, 75(2):93-104.
- 426 [8] Chugh YP, Patwardhan A. Mine-mouth power and process steam generation using fine coal waste fuel,  
427 *Resources Conservation & Recycling* , 40 (2004), pp.225–43.
- 428 [9] Zhou, C.C., et al. Transformation behavior of mineral composition and trace elements during coal gangue  
429 Combustion, *Fuel* 97 (2012), pp.644–650
- 430 [10] Xiao H.M., Ma X.Q., Co-combustion kinetics of sewage sludge with coal and coal gangue  
431 under different atmospheres, *Energy Conversion & Management*, 51 (2010),10, pp.1976–1980
- 432 [11] Frias M., et al., Effect of activated coal mining wastes on the properties of blended cement. *Cement*  
433 *Concrete Composites* 34(2012) ,5, pp. 678–683
- 434 [12] Hao, Z.F., et al., The Mineralogical Analysis and Thermal Activation Research on Coal Gangue of Zhungeer  
435 Laosangou Coalfield. *Bulletin of the Chinese Ceramic Society*, 35(2016),4, pp.1198-1199
- 436 [13] Li, C., et al., Investigation on the activation of coal gangue by a new compound method. *Journal of*  
437 *Hazardous Materials*, 179(2010), 1-3, pp.515-520
- 438 [14] Li, Z., et al., Preparation and characterization of glass–ceramic foams with waste quartz sand and coal  
439 gangue in different proportions. 23(2015), 1, pp .231–238
- 440 [15] Zhang S.G., et al., Study On Mineralogical Characteristics Of Coal gangue In The Central Area Of Hnnan,  
441 *Hunan Geology* 22(2003), 2, pp.96-100
- 442 [16] Zhang, Y.Y., et al., Effects of chemistry and mineral on structural evolution and chemical reactivity of coal  
443 gangue during calcination: towards efficient utilization. *Materials & Structures*. 48(2014), 9 , pp.1-15
- 444 [17] P. Cordeiro Lopes, Francisco A. Dias. Decomposition kinetics by thermogravimetry for the intercalation of  
445 kaolin with dimethylsulphoxide, *Materials Letters* 57(2003), 22–23. pp.3397-3401
- 446 [18] Matusik, J., Kłapyta, Z., Characterization of kaolinite intercalation compounds with  
447 Benzylalkylammonium chlorides using XRD, TGA/DTA and CHNS elemental analysis, *Applied Clay*  
448 *Science* 84(2013), pp.433-440
- 449 [19] Zhang Y.M., et al., Thermal behavior analysis of two bentonite samples selected from China, *Journal of*

- 
- 450 *Thermal Analysis & Calorimetry*.121(2015), 3, pp.1-9
- 451 [20] Vyas A, Iroh J. Thermal behavior and structure of clay/nylon-6 nanocomposite synthesized by in situ  
452 solution polymerization, *Journal Thermal Analysis & Calorimetry*, 117(2014), pp.39–52.
- 453 [21] Kaljuvee T., et al., Thermal behavior of some Estonian clays and their mixtures with oil shale ash additives,  
454 *Journal Thermal Analysis & Calorimetry*, 118(2014),2, pp.891–899
- 455 [22] Ji, H.P., et al., Phase transformation of coal gangue by aluminothermic reduction nitridation: Influence of  
456 sintering temperature and aluminum content, *Applied Clay Science* 101(2014), pp.94-99
- 457 [23] Zhang, Y., et al., Thermal behavior analysis of two bentonite samples selected from China, *Journal of*  
458 *Thermal Analysis & Calorimetry*, 121(2015), 3, pp.1-9
- 459 [24] Zhang Y, Guo Y, Cheng F, et al. Investigation of combustion characteristics and kinetics of coal gangue with  
460 different feedstock properties by thermogravimetric analysis[J]. *Thermochimica Acta*, 2015, 614  
461 (8):137-148.
- 462 [25] A.K. Varma, M. Kumar, V.K. Saxena, A. Sarkar, S.K. Banerjee, Petrographic controls on combustion  
463 behavior of inertinite rich coal and char and fly ash formation, *Fuels* 128 (2014) 199–209.
- 464 [26] H. Zhang, M. Zhou, C. Wang, M. Sun, M. Li, X.Y. Wei, Influence of mineral matters on the calorific value  
465 of an anthracite under oxygen bomb conditions, *Energy Fuels* 18 (2004) 1883–1887.
- 466 [27] H.M. Wang, C.F. You, Experimental investigation into the spontaneous ignition behavior of upgraded coal  
467 products, *Energy Fuels* 28 (2014) 2267–2271.
- 468 [28] Bayram, H., et al., Thermal analysis of a white calcium bentonite, *Journal of Thermal Analysis & Calorim*,  
469 *101*(2010),3, pp.873–879
- 470 [29] Alex, T.C., An insight into the changes in the thermal analysis curves of boehmite with mechanical  
471 Activation, *Journal of Thermal Analysis & Calorimetry*,117 (2014), 1, pp.163-171
- 472 [30] Guzmán-Castillo, M.L.,et al, Effect of Boehmite Crystallite Size and Steaming on Alumina Properties,  
473 *Journal of Physical Chemistry B*, 105(2001), 11, pp.2099-2106
- 474 [31]Cheng, Y.F., et al Insight into the thermal decomposition of kaolinite intercalated with potassium acetate: an  
475 evolved gas analysis, *Journal of Thermal Analysis & Calorimetry*, 117(2014), 3, pp.1231-1239
- 476 [32] Cheng, H. F., et al., A new method for determining platy particle aspect ratio: A kaolinite case study,  
477 *Applied Clay Science* 97-98(2014), 8, pp. 125-131
- 478 [33] Zhou, C., et al.,Transformation behavior of mineral composition and trace elements during coal gangue  
479 combustion, *Fuel*, 97(2012), pp.644–650
- 480 [34] Z Cao,Y Cao,H Dong,J Zhang,C Sun.Effect of calcination condition on the microstructure and pozzolanic  
481 activity of calcined coal gangue.*International Journal of Mineral Processing*. 2016, 146:23-28
- 482 [35] Gao, Y.J., et al.,Preparation and characterization of a novel porous silicate material from coal gangue,  
483 *Microporous & Mesoporous Materials*, 217(2015), pp. 210-218
- 484 [36] Cheng, H. F., et al., Insight into the thermal decomposition of kaolinite intercalated with potassium acetate:  
485 an evolved gas analysis, *Journal of Thermal Analysis & Calorimetry*, 117(2014), 3, pp. 1231-1239
- 486 [37] Cao, Z., et al.,Effect of calcination condition on the microstructure and pozzolanic activity of calcined coal  
487 gangue, *International Journal of Mineral Processing*. 146(2016), pp. 23-28